Hydrol. Earth Syst. Sci. Discuss., doi:10.5194/hess-2016-152, 2016
Manuscript under review for journal Hydrol. Earth Syst. Sci.
Published: 6 April 2016

Hydrology and Earth System Sciences
Open Access
Discussions

Simulated Hydrologic Response to Projected Changes in Precipitation and Temperature in the Congo River Basin

Noel Aloysius[1] and James Saiers[2]

[1] Department of Food Agriculture & Biological Engineering and Department of Ecology, Evolution and Organismal Biology, Ohio State University, Columbus, Ohio, U.S.A.

[2] School of Forestry and Environmental Studies, Yale University, New Haven, Connecticut, U.S.A

Correspondence to: Noel Aloysius (aloysius.1@osu.edu)

Abstract

Assessing the impacts of climate change on water resources of the Congo River Basin (CRB) has attracted widespread interest; however, efforts are hindered by the lack of long-term data availability. Of particular interest to water resource planners and policy makers is the spatiotemporal variability of runoff due to the projected changes in climate. Here, with the aid of a spatially explicit hydrological model forced with precipitation and temperature projections from 25 global climate models (GCMs) under two greenhouse gas emission scenarios, we elucidate the variability in runoff in the near (2016-2035) and mid (2046-2065) 21st century compared to present. Over the equatorial, northern and southwestern CRB, models project an overall increase in precipitation and, subsequently runoff. A decrease in precipitation in the headwater regions of southeastern Congo, leads to a decline in runoff. Climate model selection plays an important role in precipitation projections, for both magnitude and direction of change. Model consensus on the magnitude and the sign (increase or decrease) of change is strong in the equatorial and northern parts of the basin, but weak in the southern basin. The multi-model approach reveals that near-term projections are not impacted by the emission scenarios. However, the mid-term projections depend on the emission scenario. The projected increase in accessible runoff (excluding flood runoff) in most parts of CRB presents new opportunities for augmenting human appropriation of water resources; at the same time, the increase in quick runoff poses new challenges. In the southeast, with the projected decrease, the challenge will be on managing the increasing demands with limited water resources.

Hydrol. Earth Syst. Sci. Discuss., doi:10.5194/hess-2016-152, 2016
Manuscript under review for journal Hydrol. Earth Syst. Sci.
Published: 6 April 2016

Hydrology and Earth System Sciences
Open Access
Discussions

1. Introduction

Sustainable management of water resources (e.g. water for food production, reliable and safe drinking water and adequate sanitation) presents immense challenges in many countries in Central Africa where the Congo River Basin (CRB) is located [*IPCC*, 2014; *UNEP*, 2011; *World Food Program*, 2014]. The economies of the nine countries that share the waters of the CRB are agriculture-based [*World Bank Group*, 2014] and, therefore, are vulnerable to the impacts of climate change. Despite the abundant water and land resources and favorable climates, the basin countries are net importers of staple food grains, and are far behind in achieving Millennium Development Goals [*Bruinsma*, 2003; *Molden*, 2007; *UNEP*, 2011]. Appropriation of freshwater resources is expected to dominate in the future as the CRB countries develop and expand their economies. At the same time, climate change related risks associated with water resources will also increase significantly [*IPCC*, 2014].

Historical, present and near-future greenhouse gas emissions in the CRB countries constitute a small fraction of global emissions; however, the impacts of climate change on water resources are expected to be severe due the region's heavy reliance on natural resources (e.g. agriculture and forestry) [*Collier et al.*, 2008; *DeFries and Rosenzweig*, 2010; *Niang et al.*, 2014]. The limited adaptation capacity in the CRB region is expected to cause severe water and food security challenges, which, in turn, can lead to ecosystem degradation and increased greenhouse gas emissions [*Gibbs et al.*, 2010; *IPCC*, 2014; *Malhi and Grace*, 2000].

Competing pressures on water resources in the CRB, including revival of rural economies (largely agriculture based), achieving millennium development goals and environmental conservation, require detailed information on the spatial and temporal variability of water balance components under different climate projection pathways. The effect of climate change on water resources can be investigated by incorporating climate change projections (e.g. precipitation and temperature) in simulation models that reliably represent the spatial and temporal variability of CRB's hydrology. Such a predictive framework could be applied to forecast changes in storage and runoff, and hence freshwater availability, under different socioeconomic pathways that affect climate trajectories.

A predictive framework of CRB hydrology is hindered by insufficient data and too few evaluations of models against available data [*Beighley et al.*, 2011; *Wohl et al.*, 2012]. Basin scale water budgets estimated from land-based and satellite-derived precipitation datasets reveal significantly different results, and model-computed stream flows show only qualitative agreement with corresponding observations [*Beighley et al.*, 2011; *Lee et al.*, 2011; *Schuol et al.*, 2008]. *Tshimanga and Hughes* [2012; 2014] recently developed a semi-distributed hydrologic model capable of simulating surface-water runoff in CRB. This work crucially identified approaches suitable for approximating runoff generation at the basin scale, although the spatial resolution of the model predictions is rather coarse for supporting regional water management and regional-planning efforts. These regional planning efforts must take into account variablity and uncertainties stemming from climate-model selection and projected greenhouse gas emissions, but with respect to hydrological modeling of the CRB these issues have been incompletely addressed.

The goals of this study are to i) develop a spatially explicit hydrology model that uses downscaled output from general circulation models (GCMs) and is suitable for simulating the spatiotemporal variability of surface-water runoff throughout the CRB; ii) test the ability of the hydrological model to reproduce historical data on CRB river discharges using both observed and GCM-simulated climate fields; (iii) quantify the sensitivity of hydrologic-model runoff predictions to GCM selection; (iv) use the hydrologic model with individual GCMs and multi-GCM ensembles to forecast near-term (2016-2035) and mid-term (2046-2065) changes in surface-water flows for two greenhouse-gas emission scenarios. We focus on the runoff projections of the hydrologic model because streams and rivers will serve as the primary sources of freshwater targeted for human appropriation [*Burney et al.*, 2013; *Molden*, 2007].

We show that the hydrologic model that is forced with bias-corrected and downscaled outputs from an ensemble of 25 GCMs and two emission scenarios reveal a range of projected changes in precipitation and runoff, and that runoff yields and dynamics are highly sensitive to GCM-forcing. The multi-model mean (MM, unweighted average of all GCMs) and the select-model mean (SM, selected GCMs based on performance in the historical period and realistic representation of certain attributes in the climate system) reveal 1-3% and 4-9% increase in precipitation and runoff, respectively in the CRB in the near-term (2016-2035) relative to reference period (1985-2005). In the mid-term (2036-2065), on the other hand, projections are GCM and emission-scenario dependent, with the high emission RCP85 scenario showing the highest increases in precipitation (2-5%) and runoff (7-14%). However, both MM and SM show decreasing precipitation and runoff patterns in the southeastern headwater regions of Congo.

Hydrol. Earth Syst. Sci. Discuss., doi:10.5194/hess-2016-152, 2016
Manuscript under review for journal Hydrol. Earth Syst. Sci.
Published: 6 April 2016

2. Materials and Methods

2.1 The Congo River Basin

The Congo River Basin, with a drainage area of 3.7 million km^2, is the second largest in the world by area and discharge (Figure 1, average discharge of ~41,000km^3/s) [*Runge*, 2007]. The basin extends from 9^{o}N in the northern hemisphere to 14^{o}S in the southern hemisphere. The longitudinal extent is 11^{o}E to 35^{o}E. Nine countries share the water resources of the basin. Nearly a third of the basin area lies north of the equator. Due to its equatorial location, the basin experiences a range of climate regimes. The northern and southern parts have a strong dry and wet seasons, while the equatorial region has a bimodal rainy season [*Bultot and Griffiths*, 1972]. Much of the rain in the northern and southern CRB is received in Jun-Jul-Aug (JJA) and Dec-Jan-Feb (DJF), respectively. The primary and secondary rainy seasons in the equatorial region are Sep-Oct-Nov (SON) and Mar-Apr-May (MAM, see [*Bultot and Griffiths*, 1972] and Supplemental Information (SI) Figure S1). The mean annual precipitation is about 1,500 mm. Rainforests occupy nearly 45% of the basin and are minimally disturbed compared to the Amazon and Southeast Asian forests. Grassland and savannah ecosystems, characterized by the presence of tall grasses, closed-canopy woodlands, low-trees and shrubs, occupy another 45% [*Adams et al.*, 1996; *Bartholomé and Belward*, 2005; *Hansen et al.*, 2008; *Laporte et al.*, 1998]. Water bodies (lakes and wetlands) occupy nearly 2% of the area, but they are concentrated mostly in the southeastern and western equatorial parts of CRB (Figure 1).

In order to compare regional patterns in precipitation and runoff, we divided the basin into four regions: i) Northern Congo (NC), ii) Equatorial Congo (EQ), iii) Southwestern Congo (SW), and iv)

Southeastern Congo (SE). The EQ region covers most of the rainforest. The SE region consists of many mostly interconnected lakes and wetlands. Most of the CRB's population is concentrated in the NC, SE and SW regions [*Center for International Earth Science Information Network (CIESIN) Columbia University et al.*, 2005].

2.2 Hydrologic model for the Congo River Basin

We used the Soil Water Assessment Tool (SWAT) [*Arnold et al.*, 1998; *Neitsch et al.*, 2011] to simulate the hydrology of the CRB for historical climate (1950-2008) and for two scenarios of future climate change. SWAT is a physically based, semi-distributed watershed-scale model that operates at a daily time step. The hydrological processes simulated include evapotranspiration (ET), infiltration, surface and subsurface flows, streamflow routing and groundwater recharge. The model has been successfully employed to simulate river basin hydrology under wide variety of conditions and to investigate climate change effects on water resources [*Faramarzi et al.*, 2013; *Krysanova and White*, 2015; *Schuol et al.*, 2008; *Trambauer et al.*, 2013; *van Griensven et al.*, 2012].

We delineated 1,575 watersheds within the CRB based on topography [*Lehner et al.*, 2008]. Each watershed consists of one stream section, where near-surface groundwater flow and overland flow accumulate before being transmitted through the stream channel to the watershed outlet. Watersheds are further divided into Hydrologic Response Units (HRUs) based on land cover (16 classes) [*Bartholomé and Belward*, 2005], soils (150 types) [*FAO/IIASA*, 2009] and topography. The runoff generated within each watershed is routed through the stream network using the variable storage routing method. The average watershed size and the number of HRUs within each watershed are 2,300 km^2 and

5, respectively. We also included wetlands and lakes as natural storage structures that regulate the hydrological fluxes at different locations within CRB (Figure 1). Detailed information is not available for the all the lakes; therefore, we incorporated the largest 16 lakes (SI Table S1).

Runoff, estimated for each HRU and aggregated at the watershed level, is generated via three pathways: overland flow, lateral subsurface flow through the soil zone and release from shallow groundwater storage. The Curve Number and a kinematic storage routing methods are used to predict the first two, and a nonlinear storage-discharge relationship is used to predict groundwater contribution (see *Arnold et al.* [1998]; *Neitsch et al.* [2011] and SI). A power law relationship is employed to simulate the lake area-volume-discharge. The potential evapotranspiration is estimated using the temperature-based Hargreaves method [*Neitsch et al.*, 2011]. The actual evapotranspiration is estimated based on available soil moisture and the evaporative demand (i.e. potential evapotranspiration) for the day. Additional details on model development are provided in the Supplementary Information.

2.3 Model simulation of historical hydrology with observed climate forcings

We ran the hydrology model for the period 1950-2008. Estimates of observed daily precipitation, and minimum and maximum temperatures needed to calculate potential evapotranspiration were obtained from the Land Surface Hydrology Group at Princeton University [*Sheffield et al.*, 2006]. In addition, measured monthly streamflows were obtained at 30 gage locations (Figure 1) that had at least 10 years of records [*Global Runoff Data Center.*, 2011; *Lempicka*, 1971; *Vorosmarty et al.*, 1998].

Hydrol. Earth Syst. Sci. Discuss., doi:10.5194/hess-2016-152, 2016
Manuscript under review for journal Hydrol. Earth Syst. Sci.
Published: 6 April 2016

Hydrology and Earth System Sciences
Open Access
Discussions

The model was calibrated using observed streamflows for the period 1950-1957 at 20 locations. The number of model parameters estimated by calibration varied from 10 to 13, depending on the location of flow gages (e.g. gages with lakes within their catchment area have more parameters). The calibration involved minimizing an objective function defined as the sum-of-squared errors between observed and simulated monthly average total discharge, baseflows (estimated by applying a baseflow separation method [*Nathan and McMahon*, 1990]) and water yield. A Gauss-Marquardt-Levenberg algorithm as implemented in a model independent parameter estimation tool [*Doherty*, 2004] was used to adjust the fitted parameters and minimize the objective function. Parameter estimation was done at two stages. First, parameters for the watersheds in the upstream gages were estimated. Then the parameters for the downstream gages were estimated. To test the calibrated model, simulated stream flows were compared to stream flows measured at the same 20 locations, but during a period outside of calibration (i.e., 1958-2008), as well as at 10 additional locations that were not used in the calibration.

2.4 Hydrologic Simulations with Simulated Climate Forcing

Historical climate simulations for the period 1950-2005 and climate projections to 2099 for two emission scenarios, medium mitigation (RCP45) and high emission (RCP85), were used as a basis to drive the hydrologic model. The RCP45 scenario employs a range of technologies and policies that stabilize radiative forcing at 4.5 Wm^{-2} by 2100, whereas the RCP85 is a business-as-usual scenario, where CO_2 emissions continue to increase and radiative forcing rises above 8.5 Wm^{-2} [*Moss et al.*, 2010; *Taylor et al.*, 2012]. We used monthly precipitation and temperature outputs provided by 25 GCMs (SI Table S2) for the Fifth Assessment (CMIP5) of the Intergovernmental Panel on Climate Change (IPCC).

Hydrol. Earth Syst. Sci. Discuss., doi:10.5194/hess-2016-152, 2016
Manuscript under review for journal Hydrol. Earth Syst. Sci.
Published: 6 April 2016

Hydrology and Earth System Sciences
Discussions

GCM outputs may exhibit biases in simulating regional climate. These biases, which are attributable to inadequate representation of physical processes by the models, prevent the direct use of GCM output in climate change studies [*Randall et al.*, 2007; *Salathé Jr et al.*, 2007; *Wood et al.*, 2004]. Hydrological assessments that use GCM computations as input inherit the biases [*Salathé Jr et al.*, 2007; *Teutschbein and Seibert*, 2012]. To mitigate this problem, we implemented a statistical method [*Li et al.*, 2010] to correct the biases in the monthly historical precipitation and temperature fields. In brief, the method employs a quantile-based mapping of cumulative probability density functions for monthly GCM outputs onto those of gridded observations in the historical period. The bias correction is extended to future projections as well.

In order to be used in the CRB's hydrologic model, the simulated monthly precipitation and temperature values must be temporally downscaled to daily values. We used the three-hourly and monthly observed historical data developed for the Global Land Data Assimilation System [*Rodell et al.*, 2004; *Sheffield et al.*, 2006] and the bias-corrected monthly simulations to generate three-hourly precipitation and temperature fields, which were subsequently aggregated to obtain daily values (see SI Methods). The hydrological model was forced with the bias-corrected and downscaled daily climate fields for the period 1950-2099. A total of 50 projections (25 RCP45 and 25 RCP85 projections) were compiled and analyzed. Results of individual and multi-model means (un-weighted average of all (MM) and selected (SM) GCM simulations) for the near-term (2016-2035) and mid-term (2046-2065) projections are presented.

3. Results and Discussion

3.1 Historical simulations

The GCM-simulated mean annual precipitation (1950-2008) of 1,450 mm/year in the CRB is in good agreement with observations. We compared the GCM simulated annual precipitation with observations within the catchment areas of 30 streamflow gage locations in the historical period (Figure 2). The modeled inter-annual variability among the climate models (vertical bars in Figure 2) lies within the range of the observed variability (horizontal bars in Figure 2). The linear-regression slope of 1.16 ($p < 0.01$, Figure 2) between the annual observed and MM show that bias-corrected precipitation is slightly over-estimated, but not significantly so. Similar conclusions are drawn for the seasonal precipitation (SI Figure S2) and within the four regions identified in Figure 1 (SI Table S3).

We compared the simulated streamflows at 30 locations with observations. The colored points (Figure 3A) compare observed mean annual runoff at the 30 gages with historical simulations (forced with observed climate), while the vertical bars show the modeled inter-annual variability. The shades of colors (from light-green to yellow and red) reveal the model's skill in simulating the monthly flows in the historical period. The Nash-Sutcliff coefficient of efficiency (NSE), a measure of relative magnitude of residual variance compared to the monthly observed streamflow variance [*Legates and McCabe*, 1999; *Nash and Sutcliffe*, 1970], varies between 0.01 and 0.86 (see color scale in Figure 3A). Seventeen of the 30 gages show NSE greater than or equal to 0.5, a subjective but commonly considered acceptable value for good model performance. Higher NSE values at locations on both sides of the equator, particularly at major tributaries (NSE ~0.60, gages 1 to 8 in Figure 1 and SI Figure S3) suggest that the model reliably predicts streamflows under different climatic conditions. High NSE values also indicate that the seasonal and annual runoff simulations, including the inter-annual variability in the historical period, are in good agreement with observations. The catchment areas of the 30 gages vary between 5,000 km^2 and 900,000 km^2 (excluding the last two downstream gages), indicating the hydrology model's skill in simulating runoff satisfactorily over a wide range in watershed areas.

Comparison of modeled runoff forced with GCM-simulated and observed climate (Figure 3B) reveals generally acceptable runoff simulations in the CRB. The black dots and red (blue) vertical bars in Figure 3B show multi-model mean and maximum (minimum) range of inter-annual variability in the 25 historical GCM simulations. The results suggest that model-data agreement in precipitation translates to similarly acceptable runoff simulations. The mean and the inter-annual variability of runoff within individual models generally lie within the variability of observed runoff.

The asymmetric seasonality and magnitude in the rainfall regimes (see SI Figure S1) exhibit strong linkages with runoff. For example, the observed peak runoff at gages 2 and 6 (Figure 1) located north and south of the equator occur near the end of the rainy seasons – during Sep-Oct and Mar-Apr, respectively (Figure 4). Augmented by flows from northern and southern tributaries (e.g. gages 1, 2, 4 and 6) and by high precipitation in the tropical equatorial watersheds during the two wet seasons (MAM and SON), the main river flows (~ downstream of gage 3 in Figure 1) show low variability (Figure 4). For example, the coefficient of variation in observed (simulated) monthly flows at the basin outlet (gage 8), northern tributary (gage 2) and southern tributary (gage 4) are 0.23 (0.24), 0.77 (0.80) and 0.40 (0.48), respectively.

Regionally, runoff in the northern (NC) and southern (SW and SE) watersheds is strongly seasonal with long dry seasons, but this is not the case in the equatorial region (Figure 5). Average watershed runoff varies between 20-70 mm during dry seasons to 100-140 mm during wet seasons in the NC, SW and SE. In the equatorial region, seasonal runoff varies between 100-150mm with the highest in SON. Overall, the precipitation-runoff ratio is about 0.30 in the CRB. The accessible runoff (excluding runoff associated with flood events), which can be appropriated for human use, is about 70% of the total runoff.

3.2 Future projections in precipitation and runoff

The near-term (2016-2035) multi-model mean (MM) change in annual precipitation in the CRB is 1% relative to the reference period 1986-2005, irrespective of the emission scenario. The mid-term (2046-2065) MM projections of annual precipitation change are 1.7% and 2.1% for RCP45 and RCP85, respectively. The inter quartile range (IQR) between model and emission scenarios vary between 1.7-2.6% in the near-term and 2.6-5.8% in the mid-term, indicating considerable variability in rainfall predictions across GCMs. The inter-model variability is larger in the mid-term, and even more so for RCP85 (SI Table S4). Figure 6A-D shows the changes in precipitation in the near- and mid-term by the MM, with indications of spatial patterns under the two emission scenarios. Although overall change in the CRB is positive, the MM shows the decreasing patterns in the southern, and parts of northern CRB.

In general, the MM predicts decreasing precipitation in the driest parts of the southern CRB (mostly in SE, but portions of SW as well). Under the RCP85 scenario, the northeastern CRB also experiences reduction in precipitation in the near-term. The areas of decreased precipitation shrink in the SE and SW in the mid-term; however, drying expands in parts of northern CRB under the two emission scenarios (Figure 6C-D). Most GCMs (>15) predict an increase in the NC, EQ and most of SW, whereas majority of them predict a decrease in the SE.

We also examined the seasonal changes in the four regions (see SI Table S4). Except in the boreal summer (JJA), precipitation in the SE region is predicted to decrease under RCP45; the change is modest under RCP85. The actual increases in the north (south) during DJF (JJA) are modest (~1mm) as these are the dry seasons. The inter-model variability (SI Table S4) also exceeds the MM in all the seasonal predictions. Notably, the variability is larger in the dry seasons (e.g. DJF predictions in the NC and JJA predictions in the SE and SW). The temporal variation is further examined using monthly climatology in the reference and near- and mid-term projection periods in Figure 7A-D, which also shows the seasonal variations in the major climate regions (e.g. the bimodal rainy season in the EQ and unimodal, but asymmetric wet-dry seasons in the NC, and SW and SE). The inter-model variability is larger in the rainy seasons under RCP85, compared to RCP45. Larger variability under RCP85 highlight that GCMs may have limited skills in simulating precipitation under high greenhouse gas emissions.

The spatial pattern of runoff change in the near- and mid-terms indicated by the MM is similar to the precipitation changes, except in the northeastern CRB (3N-9N and 24E-30E) under RCP45 (Figure 6E-H). The MM runoff projections show an increase of 5% (IQR 5-7%) and 7% (IQR 7-11%) in the near- and mid-terms under both RCPs. A reduction in runoff occurs in the SE and parts of the SE under both RCPs. The area of decreasing runoff expands in the NC under both emission scenarios in the mid-term. Although northern and equatorial CRB show an overall increase in precipitation, the decrease in runoff in certain parts in the NC and EQ is caused by reduction in seasonal precipitation (i.e. limited moisture supply) rather than an increase in ET; changes in temperature associated with the two emission scenarios are relatively uniform within the GCMs (see *Aloysius et al.* [2016], and *IPCC* [2014]). Larger reduction – up to 15% – in the SE covering most of northern Zambia is due to an overall decrease in precipitation simulated by more the half of the GCMs. The inter-model variability of runoff at monthly time scales in the four regions (Figure 7E-H) is similar to precipitation, but with a time lag. The variability is larger NC and SE compared to EQ and SW during the rainy seasons.

Runoff in the EQ region, which receives the highest precipitation (~1,600mm/year) is projected to increase between 4-7%; the increases are prominent in the secondary rainy season (MAM) than the primary (SON, SI Table S5). However, runoff that can be appropriated for human use is generated mostly in the NC, SE and SW, which at present varies from 130mm/year in SE to 250-400mm/year in the NC and SW (SI Table S3). Runoff in the SW is projected to increase by 6% and 10% in the near- and mid-terms. In the NC region, runoff is projected to increase by 2-4% in the near-term and decrease in the mid-term, due to seasonal decreases (JJA and SON) in parts of NC (see Figure 6E-F and SI Tables S5 and S6). Runoff generated in populated areas in the CRB, excluding most parts of EQ, has the potential to support human needs including water supply, sanitation, food production and hydropower; however, only a portion of the total runoff can be sustainably harnessed.

3.3 Role of multi-model ensembles

Extensive coordination provided by CMIP5 enabled all climate modeling groups to use a standard set of inputs, produce compatible historical and future model runs and provide their best outputs to the IPCC data archives; thus, the multi-model ensemble approach in climate change assessment presents an opportunity to examine outputs from a range of model structure biases, initial conditions, parameter uncertainties in climate model design, which vary within GCMs [*Stocker*, 2013; *Taylor et al.*, 2012]. Skill in simulating historical precipitation and temperature increases when outputs from different GCMs are added (*Pierce et al.* [2009] and *Pincus et al.* [2008]). Along the same line, we argue that the MM approach reduces future projection uncertainties; however, we should be able to do better with a subset of models. How different are the projections if we use randomly selected subset of models or a subset that realistically simulates certain aspects in the region of interest? First, we examine the effect of MM projections based on outputs from randomly selected models out of the 25 simulations for each RCP (SI Figure S4). Projections under this random model selection method converge to MM projections as more models are added to the pool (compare values in SI Tables S4 and S5). However, with fewer models, projections vary widely and are highly dependent on the choice of GCMs.

GCMs generally have large uncertainties in simulating precipitation in the CRB region [*Aloysius et al.*, 2016; *Washington et al.*, 2013]. We examined a subset of models (SM – M6, M7, M18, M23 and M24, see refs. *Giorgetta et al.* [2013]; [*Good et al.*, 2012; *Jungclaus et al.*, 2013]; *Meehl et al.* [2013]; *Siam et al.* [2013]; *Voldoire et al.* [2012]; *Yukimoto et al.* [2006] and *Aloysius et al.* [2016] for further comparison of GCM performance) that reliably simulate regional climate as well as large-scale mechanisms that modulate regional climate. Based on diagnostic analyses to identify processes related to biases in atmospheric moisture and soil water balance in the CRB region, *Siam et al.* [2013] identifies few models in SM as good candidates for climate change assessment.

Focusing on the NC, SE and SW regions, where human appropriation of runoff is expected to increase, we find that the magnitude of annual projections (both precipitation and runoff) in SM are twice that of MM in the northern region; and the extent of drying in the south is concentrated in the southern upstream watersheds. From the viewpoint of water resources for human appropriation, the changes by seasons are also important. In Figure 8, we highlight the projections in precipitation and runoff for these regions for annual and four seasons in the form of box-and-whicker plots. Both MM and SM means reveal that the projections under RCP45 are slightly higher than RCP85 in NC region, and not so in other regions. Projection uncertainties are the largest in the dry seasons (DJF in the NC and JJA in SW and SE). Figure 8 also shows moderate increase in the SW to decrease or no-change in the SE during the rainy season (DJF). Our estimates also reveal that the upstream watersheds in the SE and parts of SW are projected to get drier with decreasing runoff (SI Table S6).

Only part of the runoff may be appropriated for human use. In the CRB, the accessible runoff, excluding runoff associated with flood events, is nearly 70%. Overall, the MM reveals a slightly higher increase in accessible runoff (5% and 7% for near- and mid-terms for both RCPs), compared to quick/flood runoff (3% in the near-term and 5-7% in the mid-term); the increase in the SM are nearly twice that of MM. However, increase in flood runoff is nearly twice that of accessible runoff in the NC region. On the other hand, both SM and MM consistently project drying in the southeastern and northeastern headwater regions (see SI Table S6).

Rural population relies on runoff from the nearby streams for water supply. The impacts on rural livelihoods due the changes in runoff are multifaceted. On the one hand, the increases in accessible runoff enhance access to water resources; on the other hand, the increases in quick/flood runoff present additional adaptation challenges. With reduced access to water resources, the impacts on rural livelihoods and the environment in the SE and parts of NC will be severe. Further, we emphasize that

GCM-related variability in regional climate change predictions can be constrained by a subset of models based on attributes that modulate large-scale circulations which, in turn affect regional climate (see *Knutti and Sedlacek* [2013] and *Masson and Knutti* [2011]). This approach is particularly useful, since regions like the CRB lack observational data; however, the mechanisms that moderate the climate system, particularly precipitation are fairly well understood [*Hastenrath*, 1984; *Nicholson and Grist*, 2003; *Washington et al.*, 2013].

3.4 Variability in accessible flows

Accessible flows (AF), which exclude flows associated with flood events (see SI Methods), are largely under-utilized in the CRB, but their appropriation is expected to increase in the future, mostly in the NC, SW and SE. We attempt to elucidate the uncertainty associated with climate model and scenario selection by quantifying seasonal and inter-model variability in AF. The seasonal variation of AF at eight major tributaries (identified in Figure 1) reveals substantial inter-model spread in the near-term (Figure 9); the model spread widens in the mid-term (SI Figure S5). The inter-model spread is large during the rainy seasons, in some cases the increase/decrease is over 50% compared to the reference period. The inter-model consensus is strong in most of the northern and southwestern tributaries (e.g. gages 1 and 6) where majority of the GCMs predict increasing precipitation. In contrast, the consensus is weak in the southeastern tributaries (e.g. gage 4). The AF in the main river (gages 3 and 8) is projected to increase in the two rainy seasons and as well as in the dry season (JJA). A close look at tributaries in the NC and SW reveal a weaker agreement on increased AF in the wet season, but a stronger agreement in the dry season (compare gages 1, 2, 6 and 7 in Figure 8). Our results also show that the decrease in precipitation and AF in SE will have marginal effect on downstream flows in the main river.

The spatial and temporal variations in the projected AF will have consequences in water resources development and management. For example, uncertainty in predicting the AF near the proposed Grand Inga Hydropower project (near gage 8, *Showers* [2009]) is low compared the predictions near the proposed trans boundary water diversion in the southeast (near gage 5, *Lund et al.* [2007]). Reductions in high and low flows in streams in the SE region will have implications on aquatic life, channel maintenance and lake and wetland flooding.

4. Conclusions

From the point of view of climate change adaptation related to water resources, agriculture, land and ecosystem management, the challenge faced by CRB countries is recognizing the value of making timely decisions in the absence of complete knowledge. To be of use to planners, the spatial and temporal variability of hydro-climatic change in the CRB is presented with sufficient details. Our analyses highlight that precipitation and runoff changes under business-as-usual and avoided greenhouse gas emission scenarios (RCP85 vs. RCP45) are rather similar in the near-term, but deviate in the mid-term, which underscores the need for rapid action on climate change adaptation. Development and implementation of adaptation strategies are often connected with large investments. Precipitation projections by GCMs, and subsequently runoff projections reveal considerable differences, which necessitate the need for multi-model evaluations of climate change impacts. With the focus on runoff – often the primary and easily accessible source of water, we show that accessible water resources increases in most parts of the CRB, with the exception in the southeast and parts of northeast.

Hydrol. Earth Syst. Sci. Discuss., doi:10.5194/hess-2016-152, 2016
Manuscript under review for journal Hydrol. Earth Syst. Sci.
Published: 6 April 2016

Comparing the MM and SM projections, the increase in runoff in the mid-term are higher under RCP85 (7-14%) than RCP45 (6-10%), however, both accessible and flood runoffs are increasing. The projected increases in accessible runoff present new opportunities to meet the increasing demands (e.g. drinking water, food production and sanitation), while the enhanced flood runoff poses new challenges. On the other hand, water managers will face different challenges in the southeast where precipitation and runoff are projected to decrease. The analyses presented in our work increase the degree of confidence in using the results for policy and management.

Acknowledgements

We would like to thank Nadine Laporte, Innocent Liengola, Peter Umunay, Greg Fiske and Melanie Burr for help with data and literature search. We acknowledge the World Climate Research Program's Working Group on Coupled Modeling, which is responsible

for CMIP, and we thank the climate modeling groups (listed in SI Table 2) for producing and making available their model output. For CMIP, the U.S. Department of Energy's

Program for Climate Model Diagnosis and Intercomparison provides coordinating support and led development of software infrastructure in partnership with the Global Organization for Earth System Science Portals. This work was supported in part by the facilities and staff of the Yale University Faculty of Arts and Sciences High Performance Computing Center, and by the National Science Foundation under grant CNS 08-21132 that partially funded acquisition of the facilities.

Hydrol. Earth Syst. Sci. Discuss., doi:10.5194/hess-2016-152, 2016
Manuscript under review for journal Hydrol. Earth Syst. Sci.
Published: 6 April 2016

References

Adams, W. M., A. Goudie, and A. R. Orme (1996), *The physical geography of Africa*, Oxford University Press, Oxford; New York.

Aloysius, N., J. Sheffield, J. E. Saiers, H. Li, and E. F. Wood (2016), Evaluation of Historical and Future Simulations of Precipitation and Temperature in Central Africa from CMIP5 Climate Models, *Journal of Geophysical Research - Atmospheres*, *121*(1), 130-152.

Arnold, J. G., R. Srinivasan, R. S. Muttiah, and J. R. Williams (1998), Large area hydrologic modeling and assessment part I: Model development, *Journal of the American Water Resources Association*, *34*(1), 73-89.

Bartholomé, E., and A. S. Belward (2005), GLC2000: a new approach to global land cover mapping from Earth observation data, *International Journal of Remote Sensing*, *26*(9), 1959-1977.

Beighley, R. E., R. L. Ray, Y. He, H. Lee, L. Schaller, K. M. Andreadis, M. Durand, D. E. Alsdorf, and C. K. Shum (2011), Comparing satellite derived precipitation datasets using the Hillslope River Routing (HRR) model in the Congo River Basin, *Hydrological Processes*, *25*(20), 3216-3229.

Bruinsma, J. (2003), *World agriculture: towards 2015/2030: an FAO perspective*, 520 pp., Earthscan/James & James, London, UK.

Bultot, F., and J. F. Griffiths (1972), The Equatorial Wet Zone, in *Climate of Africa*, edited by J. F. Griffiths, pp. 259-291, Elsevier Publishing Company, Amsterdam.

Burney, J. A., R. L. Naylor, and S. L. Postel (2013), The case for distributed irrigation as a development priority in sub-Saharan Africa, *Proceedings of the National Academy of Sciences*, *110*(31), 12513-12517.

Center for International Earth Science Information Network (CIESIN) Columbia University, United Nations Food and Agriculture Programme (FAO), and C. I. d. A. T. (CIAT) (2005), Gridded Population of the World: Future Estimates (GPWFE), edited, Center for International Earth Science Information Network (CIESIN) Columbia University, New York, United States.

Collier, P., G. Conway, and T. Venables (2008), Climate change and Africa, *Oxford Review of Economic Policy*, *24*(2), 337-353.

DeFries, R., and C. Rosenzweig (2010), Toward a whole-landscape approach for sustainable land use in the tropics, *Proceedings of the National Academy of Sciences*, *107*(46), 19627-19632.

Doherty, J. (2004), *PEST: Model-independent Parameter Estimation, User Manual Fifth Edition*, Watermark Numerical Computing, Brisbane, Australia.

FAO/IIASA (2009), Harmonized World Soil Database (version 1.1), in *Food and Agricultural Organization and IIASA*, edited, Rome, Italy and Laxenburg, Austria.

Faramarzi, M., K. C. Abbaspour, S. Ashraf Vaghefi, M. R. Farzaneh, A. J. B. Zehnder, R. Srinivasan, and H. Yang (2013), Modeling impacts of climate change on freshwater availability in Africa, *Journal of Hydrology*, *480*(0), 85-101.

Gibbs, H. K., A. S. Ruesch, F. Achard, M. K. Clayton, P. Holmgren, N. Ramankutty, and J. A. Foley (2010), Tropical forests were the primary sources of new agricultural land in the 1980s and 1990s, *Proceedings of the National Academy of Sciences*, *107*(38), 16732-16737.

Giorgetta, M. A., et al. (2013), Climate and carbon cycle changes from 1850 to 2100 in MPI-ESM simulations for the coupled model intercomparison project phase 5, *Journal of Advances in Modeling Earth Systems*, *5*(3), 572-597.

Global Runoff Data Center. (2011), Long-Term Mean Monthly Discharges and Annual Characteristics of GRDC Stations, edited by G. R. D. Center., Federal Institute of Hydrology, Koblenz, Germany.

Good, P., C. Jones, J. Lowe, R. Betts, and N. Gedney (2012), Comparing tropical forest projections from two generations of Hadley Centre Earth System models, HadGEM2-ES and HadCM3LC, *Journal of Climate*, *in press*.

Hansen, M. C., D. P. Roy, E. Lindquist, B. Adusei, C. O. Justice, and A. Altstatt (2008), A method for integrating MODIS and Landsat data for systematic monitoring of forest cover and change in the Congo Basin, *Remote Sensing of Environment*, *112*(5), 2495-2513.

Hastenrath, S. (1984), Interannual variability and annual cycle: mechanisms of circulation and climate in the tropical Atlantic sector, *Monthly Weather Review*, *112*(6), 1097-1107.

IPCC (2014), Summary for policymakers. In: Climate Change 2014: Impacts, Adaptation, and Vulnerability. Part A: Global and Sectoral Aspects. Contribution of Working Group II to the Fifth Assessment Report of the Intergovernmental Panel on Climate Change*Rep.*, 1-32 pp, Intergovernmental Panel on Climate Change, Cambridge, UK.

Jungclaus, J. H., N. Fischer, H. Haak, K. Lohmann, J. Marotzke, D. Matei, U. Mikolajewicz, D. Notz, and J. S. von Storch (2013), Characteristics of the ocean simulations in the Max Planck Institute Ocean Model (MPIOM) the ocean component of the MPI-Earth system model, *Journal of Advances in Modeling Earth Systems*, *5*(2), 422-446.

Knutti, and J. Sedlacek (2013), Robustness and uncertainties in the new CMIP5 climate model projections, *Nature Clim. Change*, *3*, 369–373.

Krysanova, V., and M. White (2015), Advances in water resources assessment with SWAT—an overview, *Hydrological Sciences Journal*, *60*(5), 771-783.

Laporte, N. T., S. J. Goetz, C. O. Justice, and M. Heinicke (1998), A new land cover map of central Africa derived from multi-resolution, multi-temporal AVHRR data, *International Journal of Remote Sensing*, *19*(18), 3537-3550.

Lee, H., R. E. Beighley, D. Alsdorf, H. C. Jung, C. K. Shum, J. Duan, J. Guo, D. Yamazaki, and K. Andreadis (2011), Characterization of terrestrial water dynamics in the Congo Basin using GRACE and satellite radar altimetry, *Remote Sensing of Environment*, *115*(12), 3530-3538.

Hydrol. Earth Syst. Sci. Discuss., doi:10.5194/hess-2016-152, 2016
Manuscript under review for journal Hydrol. Earth Syst. Sci.
Published: 6 April 2016

Legates, D. R., and G. J. McCabe, Jr. (1999), Evaluating the Use of "Goodness-of-Fit" Measures in Hydrologic and Hydroclimatic Model Validation, *Water Resour. Res.*, *35*(1), 233-241.

Lehner, H., K. Verdin, and A. Jarvis (2008), New Global Hydrography Derived from Spaceborne Elevation Data, *Eos. Trans. AGU*, *89*(10).

Lempicka, M. (1971), Bilan hydrique du bassin du fleuve Zaire. *Rep.*, Office National de la Recherche et du Development, Kinshasa, DRC.

Li , H., J. Sheffield, and E. F. Wood (2010), Bias correction of monthly precipitation and temperature fields from Intergovernmental Panel on Climate Change AR4 models using equidistant quantile matching, *J. Geophys. Res.*, *115*(D10), D10101.

Lund, B., E. Snell, D. Easton, and A. De Beer (2007), Aqueduct to link Central Africa with Southern Africa? A brief outline, *Civil Engineering = Siviele Ingenieurswese*, *15*(10), 4-8.

Malhi, Y., and J. Grace (2000), Tropical forests and atmospheric carbon dioxide, *Trends in Ecology & Evolution*, *15*(8), 332-337.

Masson, D., and R. Knutti (2011), Climate model genealogy, *Geophysical Research Letters*, *38*(8), L08703.

Meehl, G. A., W. M. Washington, J. M. Arblaster, A. Hu, H. Teng, J. E. Kay, A. Gettelman, D. M. Lawrence, B. M. Sanderson, and W. G. Strand (2013), Climate Change Projections in CESM1(CAM5) Compared to CCSM4, *Journal of Climate*, *26*(17), 6287-6308.

Molden, D. (Ed.) (2007), *Water for food, water for life : a comprehensive assessment of water management in agriculture*, 645 pp., Earthscan and International Water Management Institute, London, UK and Colombo, Sri Lanka.

Moss, R. H., et al. (2010), The next generation of scenarios for climate change research and assessment, *Nature*, *463*(7282), 747-756.

Nash, J. E., and J. V. Sutcliffe (1970), River flow forecasting through conceptual models, Part I. A discussion of principles, *Journal of Hydrology*, *10*(3), 282-290.

Nathan, R. J., and T. A. McMahon (1990), Evaluation of automated techniques for base flow and recession analyses, *Water Resources Research*, *26*(7), 1465-1473.

Neitsch, S. L., J. G. Arnold, J. R. Kiniry, and J. R. Williams (2011), Soil Water Assessment Tool - Theoretical Documentation - Version 2009*Rep. 406*, 647 pp, Texas Water Resources Institute, Texas A&M University, Temple, Texas.

Niang, I., O. C. Ruppel, M. A. Abdrabo, A. Essel, C. Lennard, J. Padgham, and P. Urquhart (2014), Africa, in *Climate Change 2014: Impacts, Adaptation, and Vulnerability. Part B: Regional Aspects. Contribution of Working Group II to the Fifth Assessment Report of the Intergovernmental Panel of Climate Change*, edited by V. R. Barros, et al., pp. 1-115, Cambridge University Press, Cambridge, United Kingdom and New York, NY, USA.

Hydrol. Earth Syst. Sci. Discuss., doi:10.5194/hess-2016-152, 2016
Manuscript under review for journal Hydrol. Earth Syst. Sci.
Published: 6 April 2016

Nicholson, S. E., and J. P. Grist (2003), The Seasonal Evolution of the Atmospheric Circulation over West Africa and Equatorial Africa, *Journal of Climate*, *16*(7), 1013-1030.

Pierce, D. W., T. P. Barnett, B. D. Santer, and P. J. Gleckler (2009), Selecting global climate models for regional climate change studies, *Proceedings of the National Academy of Sciences*, *106*(21), 8441-8446.

Pincus, R., C. P. Batstone, R. J. P. Hofmann, K. E. Taylor, and P. J. Glecker (2008), Evaluating the present-day simulation of clouds, precipitation, and radiation in climate models, *J. Geophys. Res.*, *113*(D14), D14209.

Randall, D. A., et al. (2007), Cilmate Models and Their Evaluation, in *Climate Change 2007: The Physical Science Basis. Contribution of Working Group I to the Fourth Assessment Report of the Intergovernmental Panel on Climate Change*, edited by S. Solomon, D.Qin, M. Manning, Z. Chen, M. Marquis, K. B. Averyt, M.Tignor and H. L. Miller, Cambridge University Press, Cambridge, United Kingdom and New York, NY, USA.

Rodell, M., et al. (2004), The Global Land Data Assimilation System, *Bulletin of the American Meteorological Society*, *85*(3), 381-394.

Runge, J. (2007), The Congo River, Central Africa, in *Large Rivers: Geomorphology and Management*, edited by A. Gupta, pp. 293-309, John Wiley, Chichester, England.

Salathé Jr, E. P., P. W. Mote, and M. W. Wiley (2007), Review of scenario selection and downscaling methods for the assessment of climate change impacts on hydrology in the United States pacific northwest, *International Journal of Climatology*, *27*(12), 1611-1621.

Schuol, J., K. C. Abbaspour, H. Yang, R. Srinivasan, and A. J. B. Zehnder (2008), Modeling blue and green water availability in Africa, *Water Resources Research*, *44*, W07406.

Sheffield, J., G. Goteti, and E. F. Wood (2006), Development of a 50-year high-resolution global dataset of meteorological forcings for land surface modeling, *Journal of Climate*, *19*(13), 3088-3111.

Showers, K. (2009), Congo River's Grand Inga hydroelectricity scheme: linking environmental history, policy and impact, *Water Hist*, *1*(1), 31-58.

Siam, M. S., M.-E. Demory, and E. A. B. Eltahir (2013), Hydrological Cycles over the Congo and Upper Blue Nile Basins: Evaluation of General Circulation Model Simulations and Reanalysis Products, *Journal of Climate*, *26*(22), 8881-8894.

Stocker, T. F., D. Qin, G.-K. Plattner, L.V. Alexander, S.K. Allen, N.L. Bindoff, F.-M. Bréon, J.A. Church, U. Cubasch, S. Emori, P. Forster, P. Friedlingstein, N. Gillett, J.M. Gregory, D.L. Hartmann, E. Jansen, B. Kirtman, R. Knutti, K. Krishna Kumar, P. Lemke, J. Marotzke, V. Masson-Delmotte, G.A. Meehl, I.I. Mokhov, S. Piao, V. Ramaswamy, D. Randall, M. Rhein, M. Rojas, C. Sabine, D. Shindell, L.D. Talley, D.G. Vaughan, S.-P. Xie (2013), Technical Summary. In: Climate Change 2013: The Physical Science Basis. Contribution of Working Group I to the Fifth Assessment Report of the Intergovernmental Panel on Climate Change*Rep.*, 1-84 pp, Intergovernmental Panel on Climate Change, Cambridge, UK.

Hydrol. Earth Syst. Sci. Discuss., doi:10.5194/hess-2016-152, 2016
Manuscript under review for journal Hydrol. Earth Syst. Sci.
Published: 6 April 2016

Taylor, R. Stouffer, and G. Meehl (2012), An overview of CMIP5 and the experiment design, *Bulletin of the American Meteorological Society*, *93*(4), 485.

Teutschbein, C., and J. Seibert (2012), Bias correction of regional climate model simulations for hydrological climate-change impact studies: Review and evaluation of different methods, *Journal of Hydrology*, *456–457*(0), 12-29.

Trambauer, P., S. Maskey, H. Winsemius, M. Werner, and S. Uhlenbrook (2013), A review of continental scale hydrological models and their suitability for drought forecasting in (sub-Saharan) Africa, *Physics and Chemistry of the Earth, Parts A/B/C*, *66*(0), 16-26.

Tshimanga, R. M., and D. A. Hughes (2012), Climate change and impacts on the hydrology of the Congo Basin: The case of the northern sub-basins of the Oubangui and Sangha Rivers, *Physics and Chemistry of the Earth, Parts A/B/C*, *50–52*(0), 72-83.

Tshimanga, R. M., and D. A. Hughes (2014), Basin-scale performance of a semidistributed rainfall-runoff model for hydrological predictions and water resources assessment of large rivers: The Congo River, *Water Resources Research*, *50*(2), 1174-1188.

UNEP (2011), Water Issues in the Democratic Republic of the Congo: Challenges and Opportunities*Rep.*, United Nations Environment Program, Nairobi, Kenya.

van Griensven, A., P. Ndomba, S. Yalew, and F. Kilonzo (2012), Critical review of SWAT applications in the upper Nile basin countries, *Hydrol. Earth Syst. Sci.*, *16*(9), 3371-3381.

Voldoire, A., et al. (2012), The CNRM-CM5.1 global climate model: description and basic evaluation, *Climate Dynamics*, 1-31.

Vorosmarty, C. J., B. M. Fekete, and B. A. Tucker (1998), Global River Discharge, 1807-1991, Version 1.1 (RivDIS). Data set. Available on-line [http://www.daac.ornl.gov] from Oak Ridge National Laboratory Distributed Active Archive Center, edited, Oak Ridge, Tennessee, USA.

Washington, R., R. James, H. Pearce, W. M. Pokam, and W. Moufouma-Okia (2013), Congo Basin rainfall climatology: can we believe the climate models?, *Philosophical Transactions of the Royal Society B: Biological Sciences*, *368*(1625).

Wohl, E., et al. (2012), The hydrology of the humid tropics, *Nature Clim. Change*, *2*(9), 655-662.

Wood, A. W., L. R. Leung, V. Sridhar, and D. P. Lettenmaier (2004), Hydrologic Implications of Dynamical and Statistical Approaches to Downscaling Climate Model Outputs, *Climatic Change*, *62*(1), 189-216.

World Bank Group (2014), World Development Indicators, edited, p. accessed May 2014, World Bank Publications.

World Food Program (2014), Democratic Republic of Congo*Rep.*, 113 pp, World Food Program, Rome, Italy.

Yukimoto, S., A. Noda, A. Kitoh, M. Hosaka, H. Yoshimura, T. Uchiyama, K. Shibata, O. Arakawa, and S. Kusunoki (2006), Present-day climate and climate sensitivity in the Meteorological Research

Hydrol. Earth Syst. Sci. Discuss., doi:10.5194/hess-2016-152, 2016
Manuscript under review for journal Hydrol. Earth Syst. Sci.
Published: 6 April 2016

Hydrology and Earth System Sciences
Open Access
Discussions

Institute coupled GCM version 2.3 (MRI-CGCM2. 3), *Journal of the Meteorological Society of Japan*, *84*(2), 333-363.

Hydrol. Earth Syst. Sci. Discuss., doi:10.5194/hess-2016-152, 2016
Manuscript under review for journal Hydrol. Earth Syst. Sci.
Published: 6 April 2016

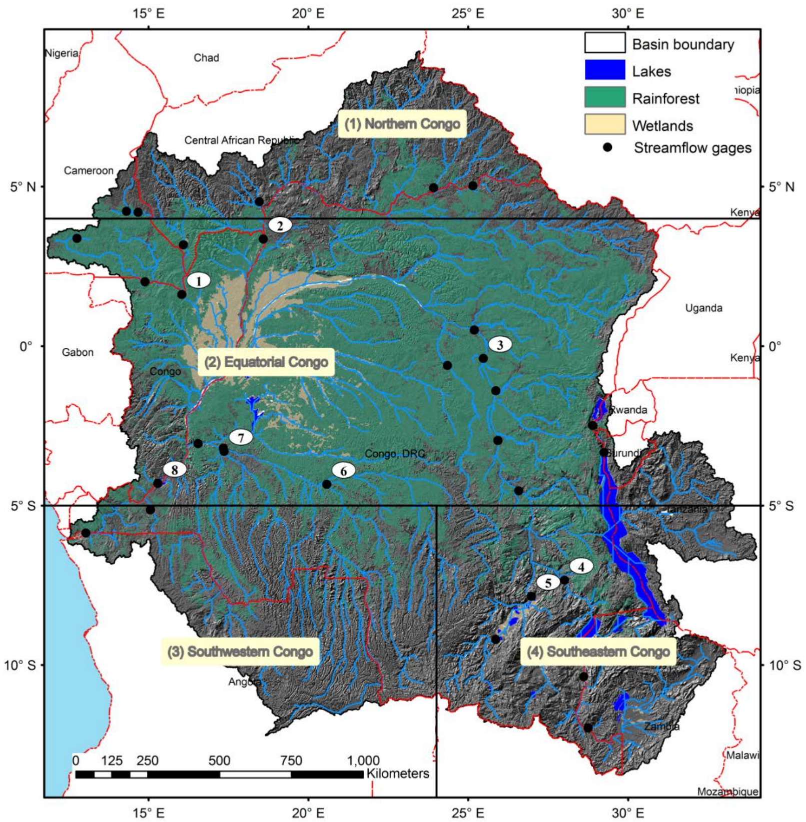

571

572 Figure 1 Congo River Basin: the river basin boundary, the extent of the rainforest, locations of lakes and wetlands, and the locations of
573 streamflow gages are shown.

Hydrol. Earth Syst. Sci. Discuss., doi:10.5194/hess-2016-152, 2016
Manuscript under review for journal Hydrol. Earth Syst. Sci.
Published: 6 April 2016

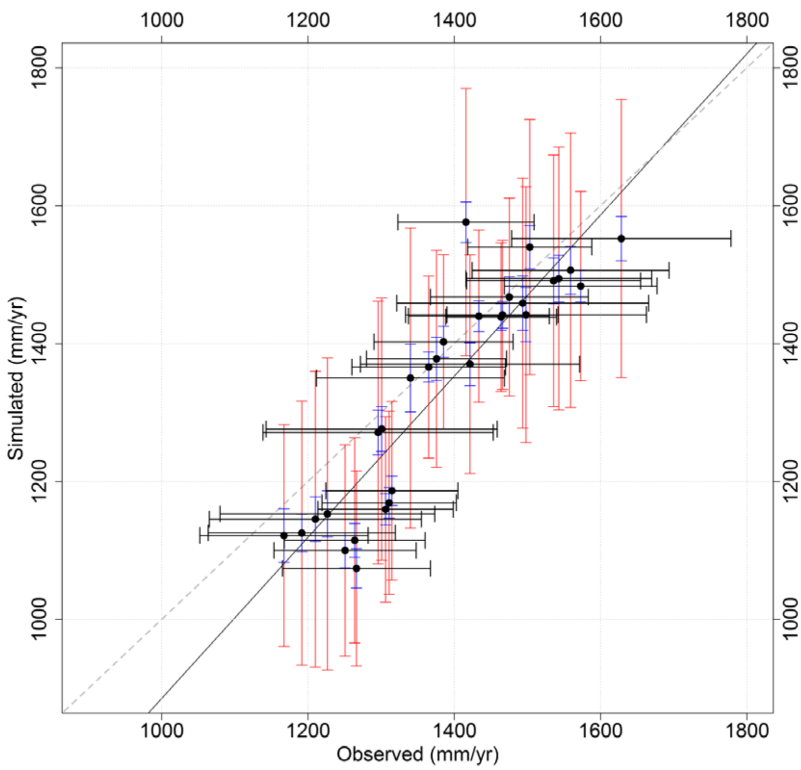

Figure 2 Comparison of observed and GCM-simulated average annual catchment precipitation at 30 gage locations (shown in Figure 1) in the historical period (1950-2005). Black dots compare multi-model means with observed precipitation, black horizontal bars show observed

Hydrol. Earth Syst. Sci. Discuss., doi:10.5194/hess-2016-152, 2016
Manuscript under review for journal Hydrol. Earth Syst. Sci.
Published: 6 April 2016

inter-annual variability, and red (blue) vertical bars show maximum (minimum) range of modeled inter-annual variability within the 25 climate model outputs.

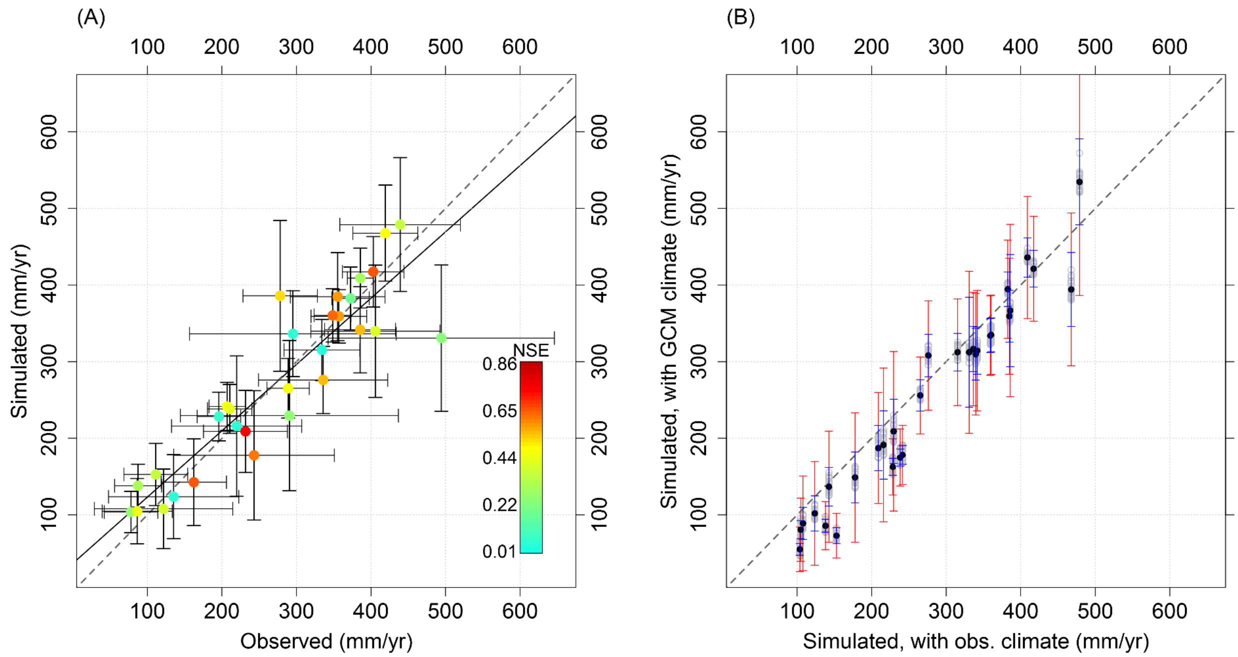

Figure 3 Comparison of observed and simulated annual water yield at the 30 streamflow gage locations (shown in Figure 1). (A) Historical simulations with observed climate: color dots compare the observed and simulated historical runoff, colored shades of the dots (see legend) shows the Nash-Sutcliff coefficient of efficiency (NSE) of observed vs. simulated monthly streamflows, black horizontal and vertical bars show observed and modeled inter-annual variability. The black line is linear regression fit between annual simulated and observed runoff ($y = 0.865 \pm 0.158x + 36.63, R^2 = 0.82, p < 0.001$), parameter bounds are the 95% confidence interval. (B) Simulations in the historical

Hydrol. Earth Syst. Sci. Discuss., doi:10.5194/hess-2016-152, 2016
Manuscript under review for journal Hydrol. Earth Syst. Sci.
Published: 6 April 2016

period with GCM-simulated climate: black dots show the multi-model mean and red (blue) vertical bars show modeled (forced with GCM-simulated historical climate) maximum (minimum) inter-annual variability within the 25 simulations, gray circles show multi-year mean of individual GCM simulations. The gray dotted lines in A and B are 1:1 fit.

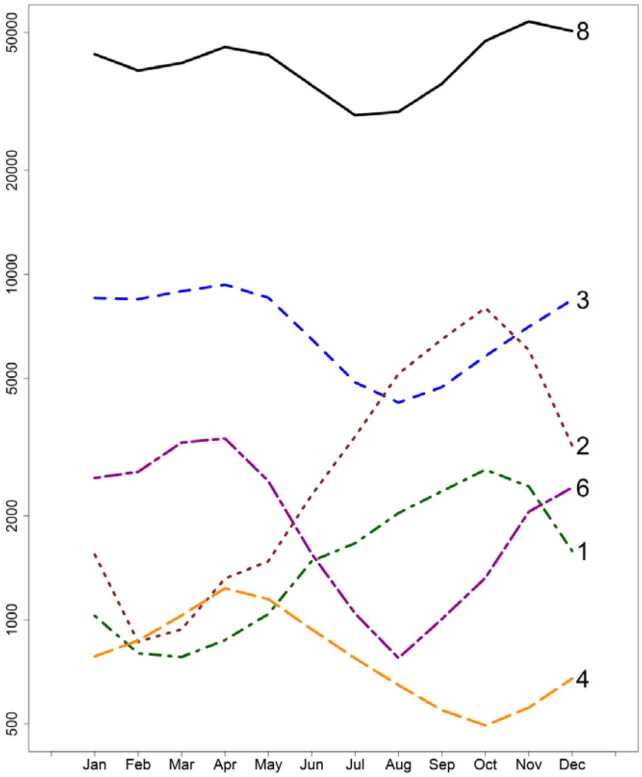

Figure 4 Mean monthly flows at selected tributaries in the CRB. Flows are in m^3/s and gage numbers are identified in Figure 1. Monthly values are based on simulated flows (forced with observed precipitation) for the period 1950-2005.

Hydrol. Earth Syst. Sci. Discuss., doi:10.5194/hess-2016-152, 2016
Manuscript under review for journal Hydrol. Earth Syst. Sci.
Published: 6 April 2016

Hydrology and Earth System Sciences
Discussions
Open Access

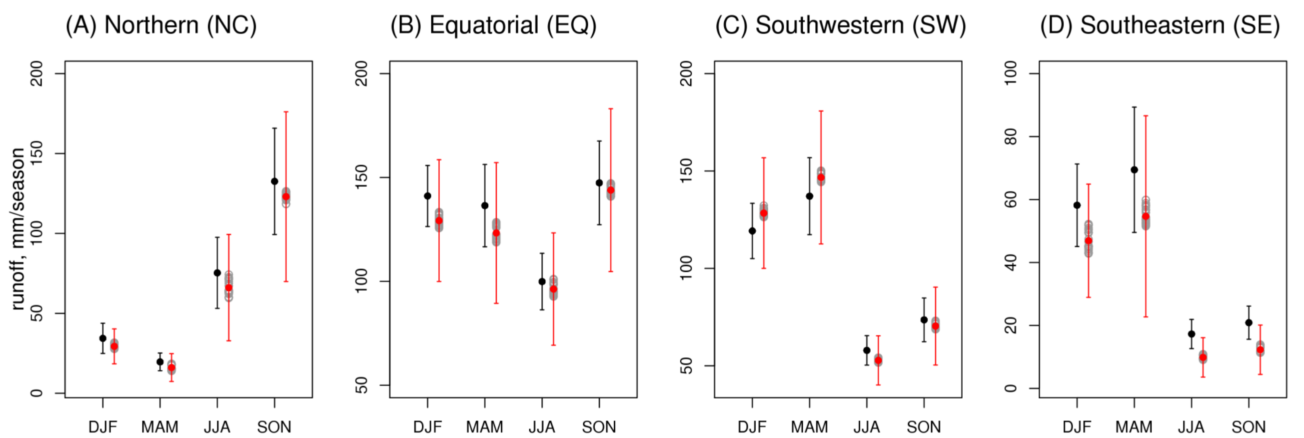

Figure 5 Seasonal variation in runoff in (A) Northern, (B) Equatorial, (C) Southwestern and (D) Southeastern Congo River Basin. Black dots and vertical bars show the modeled inter-annual variability forced with observed climate, red dots show the multi-model mean forced with GCM-simulated climate, red vertical bars show the maximum range of inter-annual variability within the 25 models and the grey open circles show the mean of individual models in the historical period, 1950-2005. Y-axis scale is different for each plot.

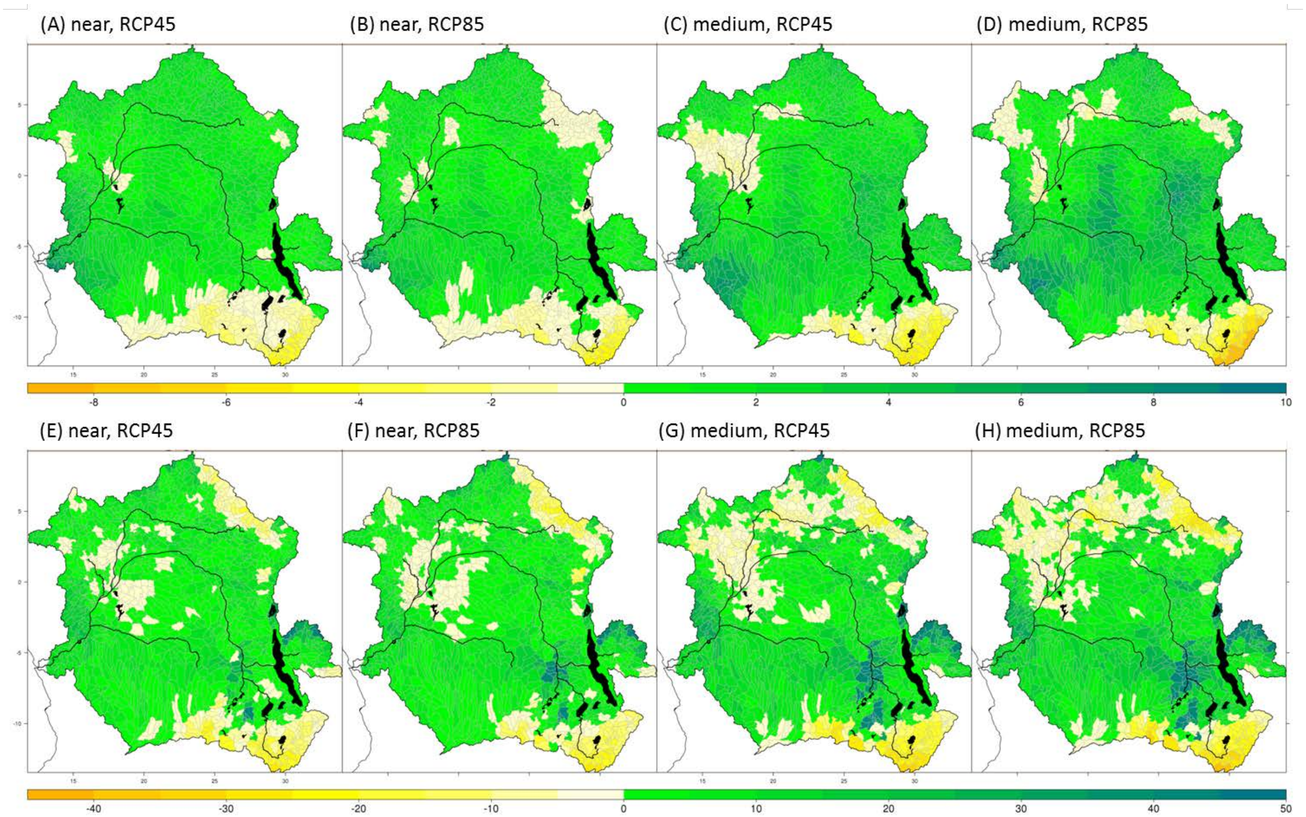
(A) near, RCP45
(B) near, RCP85
(C) medium, RCP45
(D) medium, RCP85
-8 -6 -4 -2 0 2 4 6 8 10
(E) near, RCP45
(F) near, RCP85
(G) medium, RCP45
(H) medium, RCP85
-40 -30 -20 -10 0 10 20 30 40 50

Hydrol. Earth Syst. Sci. Discuss., doi:10.5194/hess-2016-152, 2016
Manuscript under review for journal Hydrol. Earth Syst. Sci.
Published: 6 April 2016

Hydrology and Earth System Sciences Discussions
Open Access

Figure 6 Multi-model mean changes in annual precipitation (A-D) and runoff (E-H), as percentage, for near-term (2016-2035) and mid-term (2046-2065) relative to the reference period (1986-2005) under the Representative Concentration Pathways, RCP45 and RCP85. The number of GCMs to calculate the multi-model mean is 25. Main rivers and lakes are shown as black lines and polygons.

Hydrol. Earth Syst. Sci. Discuss., doi:10.5194/hess-2016-152, 2016
Manuscript under review for journal Hydrol. Earth Syst. Sci.
Published: 6 April 2016

Hydrology and Earth System Sciences
Open Access
Discussions

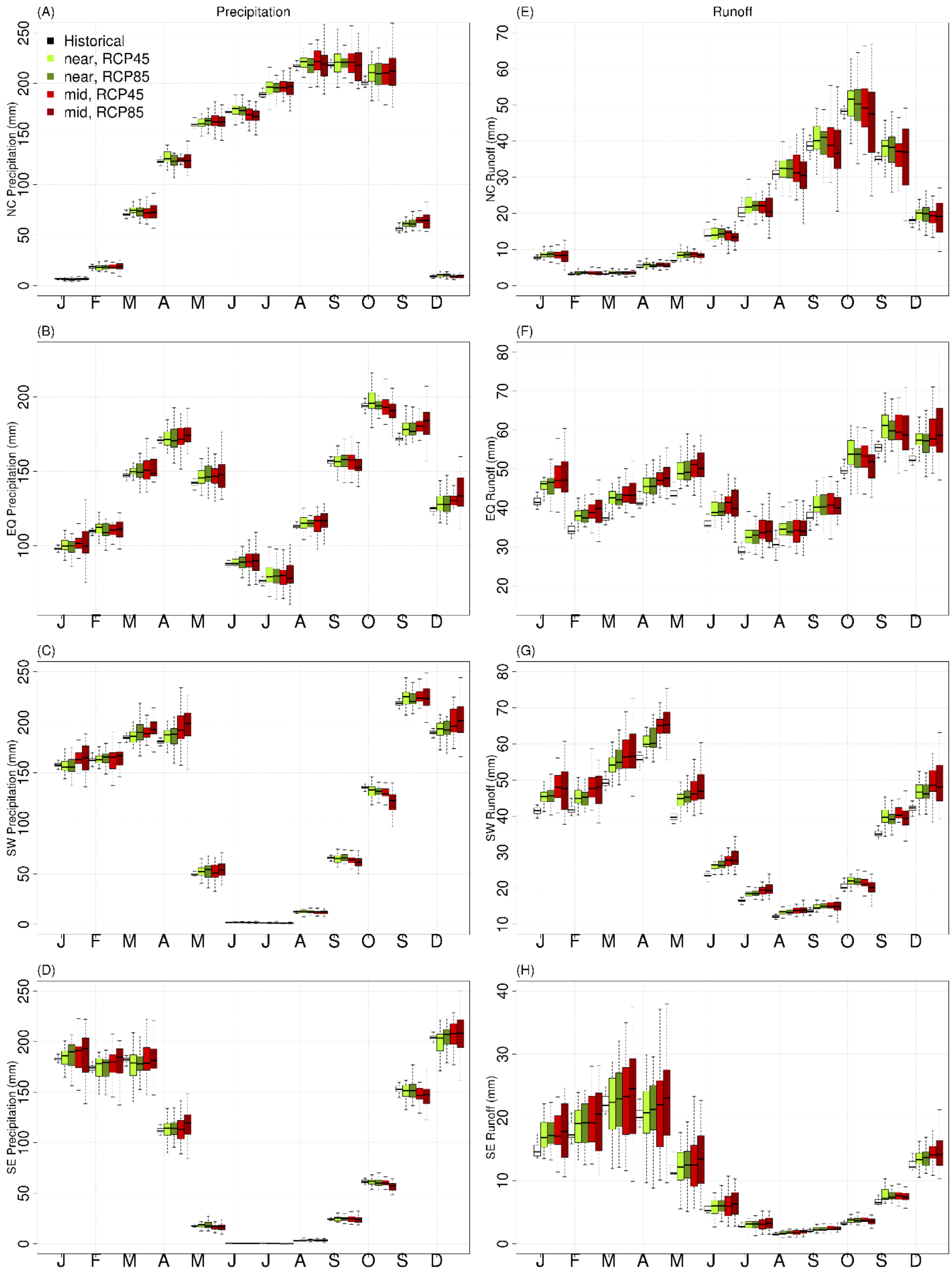

604

Hydrol. Earth Syst. Sci. Discuss., doi:10.5194/hess-2016-152, 2016
Manuscript under review for journal Hydrol. Earth Syst. Sci.
Published: 6 April 2016

Hydrology and Earth System Sciences
Open Access
Discussions

Figure 7 Monthly variation of precipitation (A-D) and runoff (E-H) in the four regions shown in Figure 1A. Box-and-whiskers for each month shows the inter-model variability for the historical period (black), near-term RCP45 (light green), near-term RCP85 (dark green), mid-term RCP45 (red) and mid-term RCP85 (brown). The upper and lower end of the boxes show the 75th and 25th quartiles, the mid bar in each box shows the median, and the outer lines cover approximately 90% of the values. All values are in mm/month.

Hydrol. Earth Syst. Sci. Discuss., doi:10.5194/hess-2016-152, 2016
Manuscript under review for journal Hydrol. Earth Syst. Sci.
Published: 6 April 2016

612

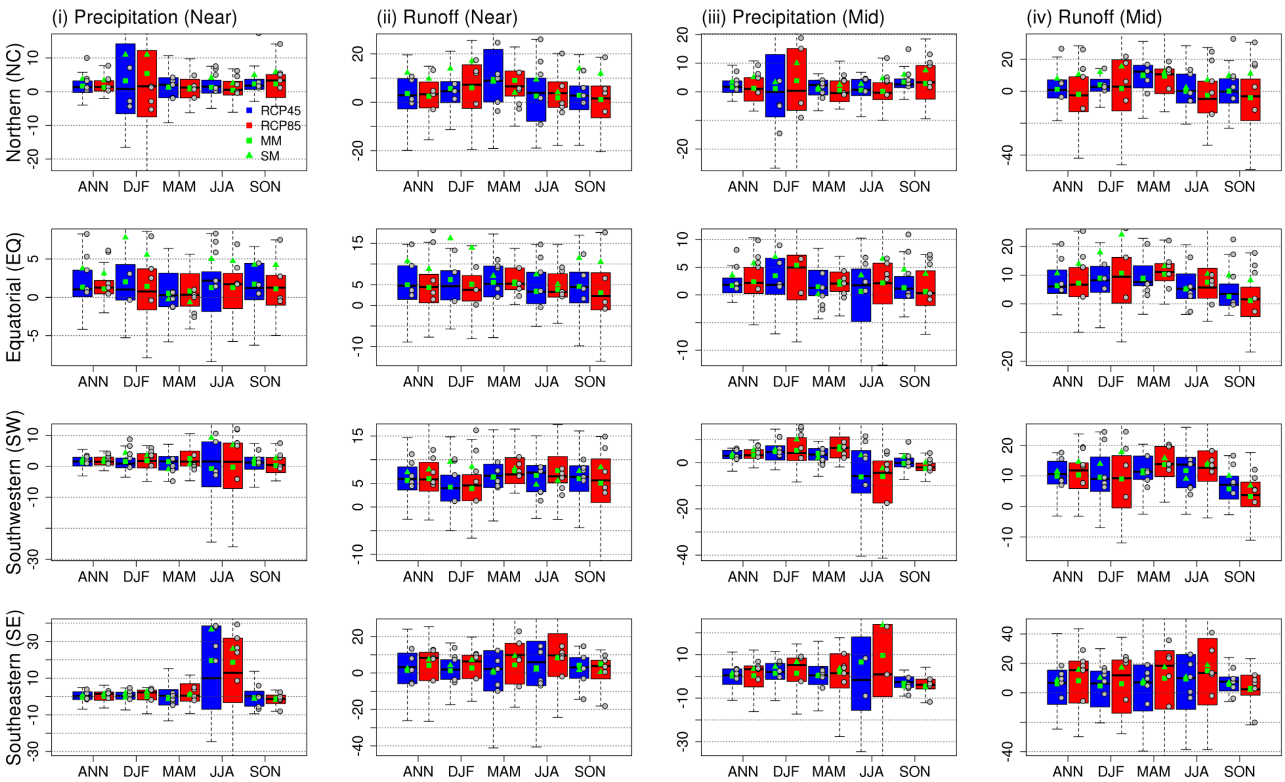

613

Hydrol. Earth Syst. Sci. Discuss., doi:10.5194/hess-2016-152, 2016
Manuscript under review for journal Hydrol. Earth Syst. Sci.
Published: 6 April 2016

Hydrology and Earth System Sciences
Discussions

Figure 8 Annual and seasonal precipitation and runoff projections (as percent relative to the reference period 1986-2005) for the northern (NC, first row), equatorial (EQ, second row), southwestern (SW, third row) and southeastern (SE, fourth row) regions. Columns (i) and (iii) are near- and mid-term precipitation projections, and columns (ii) and (iv) are runoff projections. Boxes show the 25^{th} and 75^{th} percentiles, the horizontal line within the boxes show median value and the whiskers mark the 5^{th} and 95^{th} percentiles. Green squares (triangles) indicate the MM (SM) means and the grey dots indicate individual models in the SM. All values are computed relative to the reference period 1986-2005 and reported as percentages. The y-axis range is limited to show the smaller boxes. Y-axis values are in percent.

Hydrol. Earth Syst. Sci. Discuss., doi:10.5194/hess-2016-152, 2016
Manuscript under review for journal Hydrol. Earth Syst. Sci.
Published: 6 April 2016

Hydrology and Earth System Sciences
Open Access
Discussions

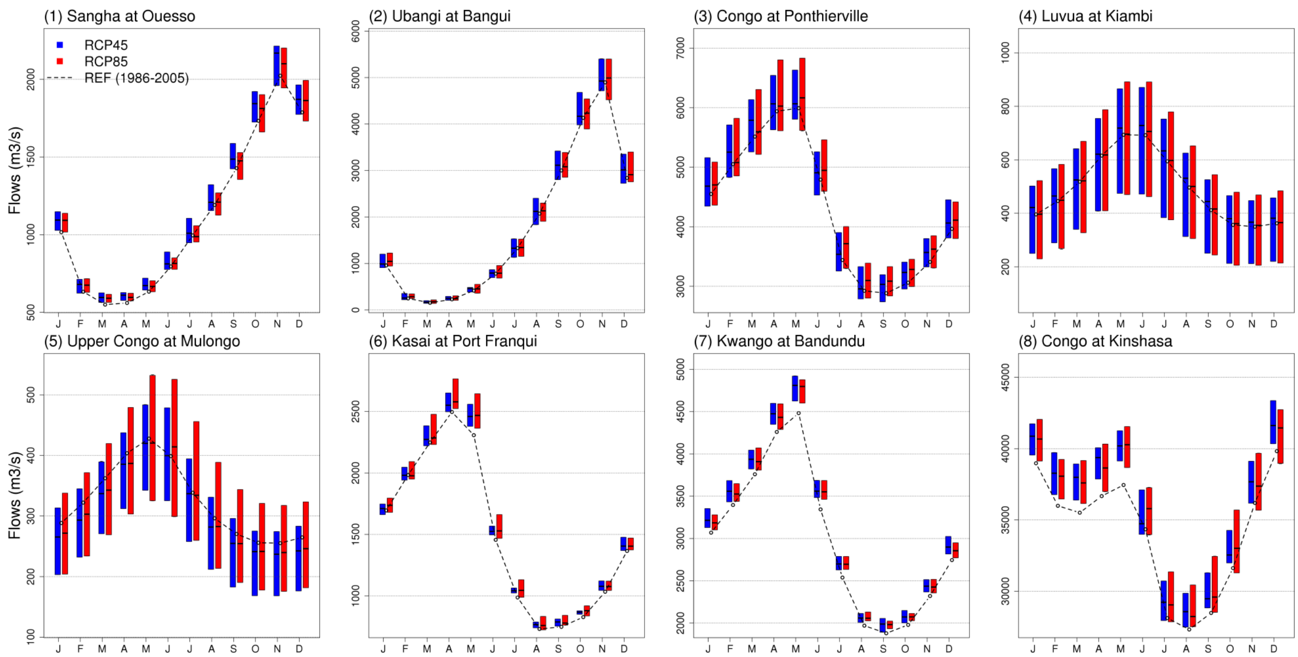

Figure 9 Accessible streamflow hydrographs in the near-term at selected locations shown in Figure 1A. Blue (red) bars show the inter-model variability. Dotted black line shows the hydrograph in the reference period (1986-2005). Figure numbers 1-8 coincide with the gage numbers in Figure 1.